Archives of Hydro-Engineering and Environmental Mechanics
Vol. 51 (2004), No. 3, pp. 205–224

Modelling of Gravity Waves in Water of Finite Depth

Włodzimierz Chybicki

Institute of Hydro-Engineering of the Polish Academy of Sciences
ul. Kościerska 7, 80-953 Gdańsk, Poland, e-mail: wchyb@ibwpan.gda.pl

(Received November 14, 2003; revised March 03, 2004)

Abstract

An extension of shallow water theory proposed by Wilde (Wilde, Chybicki 2000), for finite water depth and based on the Lagrangian type formalism is presented. As in Bussinesq-type models the vertical dimension is being eliminated and the horizontal displacement is expanded in the even power series of vertical variable *Y*, but only two terms – with power null and two are taken into account. Based on continuity equation, vertical displacement is expressed in terms of horizontal displacement and its derivatives. The equations of motion are derived from a Hamilton principle applied to Lagrangian function being a difference of kinetic and potential energy.

In order to solve the set of governing equations a direct method of variational calculus has been applied. The solutions preserve total energy. The numerical simulations have been verified experimentally, in terms of wave measurements in the flume, for various wave heights and ratios of wavelength to water depth, showing good conformity between measured and calculated values. The theory presented here can also be applied for the case of varying depth.

Key words: gravity waves, Hamilton principle, Lagrangian description

1. Introduction

Traditionally, for the solution of the problem of waves in water of finite depth, simplified equations are being incorporated. The methods usually involve perturbation procedures in which the velocity potential is expanded as a power series in a small parameter, being a ratio of wave height to wavelength. For monochromatic waves over a slowly varying depth the first order solution, or linearized theory is employed. Omitting the reflected wave energy restricts the use of theory to the very gentle topography.

Wide classes of approximations are so-called the 'vertically integrated' models, in which vertical coordinate is removed. Part of them can be obtained from the Hamiltonian principle. For the Euler description, Luke (1967) developed such a principle for the non-linear, irrotational free surface flows. The approximation of vertical structure of the fluid motion eliminates the vertical variable z from the

equation. In the simplest case in which horizontal velocity of fluid is independent of vertical variable, long wave theory can be derived. The expansion of potential function in power series of vertical variable together with consideration of first several terms only, lead to Bussinesq-type equation with weakly dispersion. There are many extensions of such approach for deeper water. Most of them are described by Dingemans (1997a, 1997b).

The assumption of the progressive wave that potential function as $\phi(x, y, z) = \varphi(x, y)\cosh(k(z+h))$, where $k = k(h)$ is the local wave-number corresponding to the local depth, leads to so-called mild-slope approximation (Chamberlain, Porter 1995).

In general, the variational principle is a powerful method serving for approximations of basic equations. The method has also been used in the presented work, however for the Lagrangian description.

In the paper presented the equations of motion are developed. The results of numerical simulations have been compared with experimental data.

2. Equations of Motion

In the problem presented here, space is treated as Euclidean and two-dimensional. It is assumed that the fluid for the time $t \leq 0$ is at rest and the corresponding particle co-ordinates are named X, Y ($0 \leq X \leq L,\ -H \leq Y \leq 0$), where L denotes length of the flume, H depth of water, and free surface elevation is described as $Y = 0$. The motion of the fluid is described by the mapping of points (X, Y) into the positions occupied by the points at time t. Thus, the mapping can be given as:

$$\begin{aligned} x &= x(X, Y, t) = X + w(X, Y, t), \\ y &= y(X, Y, t) = Y + z(X, Y, t), \end{aligned} \tag{1}$$

where $w(X, Y, t)$ and $z(X, Y, t)$ denote horizontal and vertical displacements with time t of the particles X, Y, respectively. Let us assume that these displacements can be expanded as power series of variable Y. Horizontal displacement contains only even power and vertical displacement odd power of variable Y (Ursell 1953). In addition, let us assume that horizontal displacement can be represented by two first terms of series: with power equal to zero and two:

$$\begin{aligned} x(X, Y, t) &= X + \sum_{i=1,2} x_i(X, t)\frac{Y^{2(i-1)}}{H^{2(i-1)}} = X + x_1(X, t) + x_2(X, t)\frac{Y^2}{H^2}, \\ y(X, Y, t) &= Y + \sum_{i=1,n} y_i(X, t)\frac{Y^{2i-1}}{H^{2i-1}}. \end{aligned} \tag{2}$$

A condition of the incompressibility of fluid corresponds to the statement that the Jacobian is equal to one, for all fluid material points, and at all times, i.e.:

$$\frac{\partial(x,y)}{\partial(X,Y)} = x_X y_Y - x_Y y_X = 1, \tag{3}$$

in which x_X, y_X, x_Y, y_Y denote partial derivatives of horizontal and vertical coordinates over horizontal and vertical variables respectively.

After substitution of the equation (1) into equation (2), continuity equation is expressed as power series of variable Y . Because the coefficients of every power of variable Y are zero, we can subsequently express functions $v_i(X,t)$ in terms of the relations: $u_1(X,t)$, $u_2(X,t)$, and their derivatives.

The term of the lowest order yields the following equation:

$$v_1(X,t) = \frac{-Hx_{1,X}(X,t)}{1+x_{1,X}(X,t)}. \tag{4}$$

Similarly, after some algebra the second power of Y yields:

$$v_2(X,t) = -H\frac{x_{2,X}(X,t) + x_{1,X}(X,t)x_{2,X}(X,t) + 2x_2(X,t)x_{1,XX}(X,t)}{3\left(1+x_{1,X}(X,t)\right)^3}. \tag{5}$$

Next, the components of vertical displacement $v_n(X,t)$, $n > 3$, can be expressed by recurrence formulae:

$$v_n(X,t) = \frac{-(2n-3)y_{n-1}(X,t)x_{2,X}(X,t) + 2x_2(X,t)y_{n-1,X}(X,t)}{(2n-1)(1+x_{1,X}(X,t))}. \tag{6}$$

Using the assumption (2) regarding the relations of displacements, the motion can be described only by functions $x_1(X,t)$ and $x_2(X,t)$, and continuity equation is satisfied.

Equations (4–6), restricted to second order, reduce to the following form:

$$y_1(X,t) = H\left(-x_{1,X}(X,t) + x_{1,X}^2(X,t)\right), \tag{7}$$

$$y_2(X,t) = H\left(-x_{2,X}(X,t) + 2x_{1,X}(X,t)x_{2,X}(X,t) - 2x_2(X,t)x_{1,XX}(X,t)\right)/3, \tag{8}$$

$$y_3(X,t) = H\left(-3x_{2,X}^2(X,t) - 2x_2(X,t)x_{2,XX}(X,t)\right)/15. \tag{9}$$

The equations of motion can be derived from a principle of stationary action:

$$\delta\int_t dt\, L = 0, \quad \text{where} \quad L = \int_x dx \int_y dy\, L, \tag{10}$$

with Lagrangian function equal to the difference between the kinetic and potential energy, given as:

$$L = \rho \frac{1}{2}\left(x_t^2 + y_t^2\right) - \rho g y. \tag{11}$$

After integration over vertical variable Y and restriction to the second order, we obtain:

$$L = L1 + L2,$$

where:

$$\begin{aligned} L1 &= \rho g H^2 (6x_{1,X} + x_{2,X})/12, \\ L2 &= \rho\left(\frac{Hx_{1,t}^2}{2} + \frac{Hx_{2,t}^2}{10} + \frac{H^3 x_{1,tX}^2}{6} + \frac{H^3 x_{2,tX}^2}{126} + \frac{Hx_{1,t}x_{2,t}}{3} + \right. \\ &\quad + \frac{H^3 x_{1,tX}x_{2,tX}}{15} - \frac{gH^2 x_{1,X}^2}{2} - \frac{gH^2 x_{2,X}^2}{30} - \frac{gH^2 x_{1,X}x_{2X}}{6} + \\ &\quad \left. + \frac{gH^2 x_{1,XX}x_2}{6} + \frac{gH^2 x_{2,XX}x_2}{45)}\right). \end{aligned} \tag{12}$$

The equations of motion can be determined now from stationarity of the functional:

$$\delta \int_t \int_x (L1 + L2) dx dt = 0. \tag{13}$$

Note that the potential energy, with accuracy to a total differential, can be expressed as:

$$Ep = \frac{gH^2}{2}\left(x_{1,X}^2 + \frac{1}{3}x_{2,X}\right)^2. \tag{14}$$

Variation of the functional of functions $x_1(X,t)$ and $x_2(X,t)$ yields two equations of motion:

$$\begin{aligned} &-\frac{\partial}{\partial t}\frac{\partial L}{\partial x_{1,t}} - \frac{\partial}{\partial X}\frac{\partial L}{\partial x_{1,X}} + \frac{\partial^2}{\partial X^2}\frac{\partial L}{\partial x_{1,XX}} + \frac{\partial^2}{\partial X \partial t}\frac{\partial L}{\partial x_{1,tX}} = \\ &\frac{Hx_{1,ttXX}}{3} + gH^2 x_{1,XX} - Hx_{1,tt} + \frac{Hx_{2,ttXX}}{15} - \frac{Hx_{2,tt}}{3} + \frac{gH^2 x_{2,XX}}{3} = 0, \\ &-\frac{\partial}{\partial t}\frac{\partial L}{\partial x_{2,t}} - \frac{\partial}{\partial X}\frac{\partial L}{\partial x_{2,X}} + \frac{\partial^2}{\partial X^2}\frac{\partial L}{\partial x_{2,XX}} + \frac{\partial^2}{\partial X \partial t}\frac{\partial L}{\partial x_{2,tX}} = \\ &\frac{Hx_{1,ttXX}}{15} + \frac{gH^2 x_{1,XX}}{3} - \frac{Hx_{1,tt}}{3} + \frac{Hx_{2,ttXX}}{63} - \frac{Hx_{2,tt}}{5} + \frac{gH^2 x_{2,XX}}{9} = 0. \end{aligned} \tag{15}$$

3. Dispersion Relation

Let us assume that solutions of equations (15–16) represent the progressive wave:

$$x_1(X,t) = A_1 \cos(kX - \omega t), \tag{16}$$

$$x_2(X,t) = A_2 \cos(kX - \omega t). \tag{17}$$

On such assumption, that the above equations can be expressed by a linear homogeneous system of two algebraic equations we obtain:

$$\begin{aligned} A1 \cdot H\left(gHk^2 - \omega^2 - \frac{1}{3}H^2k^2\omega^2\right) + \\ +A2 \cdot H\left(\frac{1}{3}gHk^2 - \frac{1}{3}\omega^2 - \frac{1}{15}H^2k^2\omega^2\right) = 0, \\ A1 \cdot H\left(\frac{1}{3}gHk^2 - \frac{1}{3}\omega^2 - \frac{1}{15}H^2k^2\omega^2\right) + \\ +A2 \cdot H\left(\frac{1}{9}gHk^2 - \frac{1}{5}\omega^2 - \frac{1}{63}H^2k^2\omega^2\right) = 0, \end{aligned} \tag{18}$$

which can be written as:

$$\mathbf{A} \cdot \mathbf{X} = 0, \tag{19}$$

where **A** denotes the following matrix:

$$\begin{bmatrix} H\left(gHk^2 - \omega^2 - \frac{1}{3}H^2k^2\omega^2\right) & H\left(\frac{1}{3}gHk^2 - \frac{1}{3}\omega^2 - \frac{1}{15}H^2k^2\omega^2\right) \\ H\left(\frac{1}{3}gHk^2 - \frac{1}{3}\omega^2 - \frac{1}{15}H^2k^2\omega^2\right) & H\left(\frac{1}{9}gHk^2 - \frac{1}{5}\omega^2 - \frac{1}{63}H^2k^2\omega^2\right) \end{bmatrix} \tag{20}$$

and **X** denotes the following vector:

$$\begin{bmatrix} A_1 \\ A_2 \end{bmatrix}. \tag{21}$$

This system has non-zero solution only if the determinant is equal to zero i.e.:

$$Det\ \mathbf{A} = 0. \tag{22}$$

Calculating the determinant of matrix **A**, we obtain:

$$\frac{4H^2}{4725}\omega^2\left(\omega^2(105 + 45k^2H^2 + k^4H^4) - gk(105kH + 10k^3H^3)\right) = 0. \tag{23}$$

This determinant vanishes when:

$$\omega = 0 \tag{24}$$

or

$$\omega^2 = \frac{gHk^2(105 + 10k^2H^2)}{(105 + 45k^2H^2 + k^4H^4)}. \tag{25}$$

The last equation describes dispersion relation for progressive waves. In both cases described by equations (24) and (25), assuming that equation (25) is satisfied, when the determinant is zero, both equations (18) are equivalent and the non-zero solutions are as follows:

$$\begin{aligned} &A_1 + \frac{A_2}{3} = 0 \quad \text{when} \quad \omega = 0 \\ &\text{and} \\ &A_2(14 - H^2k^2) = 7A_1H^2k^2. \end{aligned} \tag{26}$$

The comparison between dispersion relation (25) and linear dispersion relation described by:

$$\omega = \sqrt{gk\tanh(kH)}, \tag{27}$$

for $H = 1$ m is presented in Fig. 1, where dotted line denotes linear dispersion relation and solid line solution obtained by the presented theory.

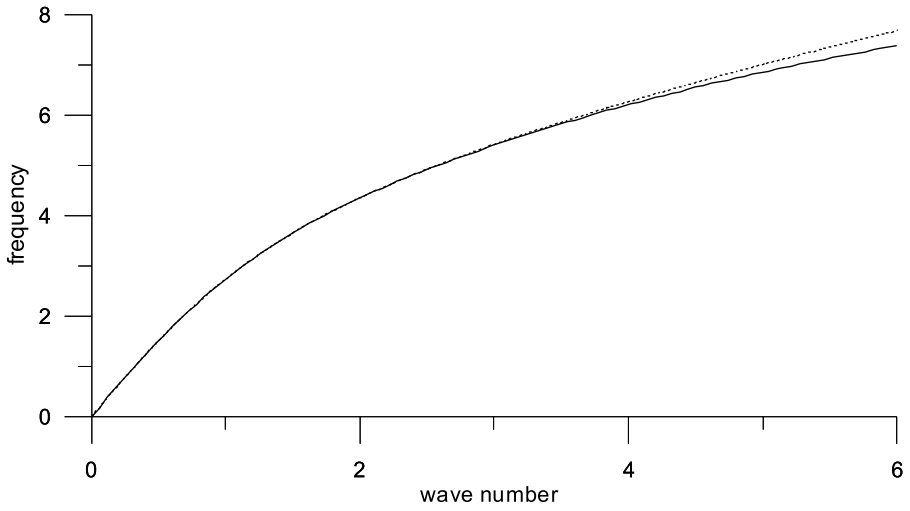

Fig. 1. Comparison between linear dispersion relation and dispersion relation described by the presented theory, for $H = 1$

4. Numerical Model

In order to solve equations (15) the finite element method has been applied. Let us consider a rectangular element of the dimensions denoted as Δt and ΔX. In the element a local coordinate system (t, X) was chosen with the origin placed in the centre of the rectangle. In action integrals exist only first order time derivatives, but second and third space derivatives, so the element must be more complicated in space. Let us express an unknown function of horizontal $x_1(X,t)$ and $x_2(X,t)$ displacements in this element as a following function:

$$x_1(X,t) = A_{11} + A_{12}X/\Delta X + A_{13}X^2/\Delta X^2 + A_{14}X^3/\Delta X^3 + t(A_{21} + A_{22}X/\Delta X + A_{23}X^2/\Delta X^2 + A_{24}X^3/\Delta X^3)/\Delta t, \tag{28}$$

$$x_2(X,t) = B_{11} + B_{12}X/\Delta X + B_{13}X^2/\Delta X^2 + B_{14}X^3/\Delta X^3 + t(B_{21} + B_{22}X/\Delta X + B_{23}X^2/\Delta X^2 + B_{24}X^3/\Delta X^3)/\Delta t, \tag{29}$$

for
$-\Delta X/2 < X < \Delta X/2,$
$-\Delta t/2 < t < \Delta t/2.$

For every function $x_1(X,t)$ and $x_2(X,t)$, the coefficients A_{ij} and B_{ij} are determined by the following relationships:

$$\begin{aligned} &x(-\Delta X/2, -\Delta t/2) = x_A(s), \quad && x(\Delta X/2, -\Delta t/2) = x_B(s), \\ &x(-\Delta X/2, \Delta t/2) = x_A(s+1), \quad && x(\Delta X/2, \Delta t/2) = x_B(s+1), \end{aligned} \tag{30}$$

$$\begin{aligned} &\frac{\partial x}{\partial X}(-\Delta X/2, -\Delta t/2) = x_A'(s), \quad && \frac{\partial x}{\partial X}(\Delta X/2, -\Delta t/2) = x_B'(s), \\ &\frac{\partial x}{\partial X}(-\Delta X/2, \Delta t/2) = x_A'(s+1), \quad && \frac{\partial x}{\partial X}(\Delta X/2, \Delta t/2) = x_B'(s+1), \end{aligned} \tag{31}$$

where quantities $x_A(s), x_B(s), x_A(s+1), x_B(s+1)$ correspond to the values of the functions at the corners of the rectangle, while quantities $x_A'(s), x_B'(s), x_A'(s+1)$, $x_B'(s+1)$ are the values of its spatial derivatives at the same points:

$$x_C'(k) = \frac{\partial x}{\partial X}_{|x=C, t=k\Delta t}.$$

The solution of this system of equations can be written in the following form:

$$A_{11} = (\Delta X[x_{1,A}'(s) + x_{1,A}'(s+1) - x_{1,B}'(s) - x_{1,B}'(s+1)] + 4[x_{1,B}(s) + x_{1,A}(s) + x_{1,A}(s+1) + x_{1,B}(s+1)])/16, \tag{32}$$

$$A_{12} = [-\Delta X(x_{1,A}'(s) + x_{1,A}'(s+1) + x_{1,B}'(s) + x_{1,B}'(s+1)] + 6[x_{1,B}(s) + x_{1,B}(s+1) - x_{1,A}(s) - x_{1,A}(s+1)])/8, \tag{33}$$

$$A_{13} = (\Delta X[-x'_{1,A}(s) - x'_{1,A}(s+1) + x'_{1,B}(s) + x'_{1,B}(s+1)])/4, \tag{34}$$

$$\begin{aligned} A_{14} = (\Delta X[&x'_{1,A}(s) + x'_{1,A}(s+1) + x'_{1,B}(s) + x'_{1,B}(s+1)] + \\ 2[&x_{1,A}(s) + x_{1,A}(s+1) - x_{1,B}(s) - x_{1,B}(s+1)])/2, \end{aligned} \tag{35}$$

$$\begin{aligned} A_{21} = (-\Delta X[&x'_{1,A}(s) + x'_{1,A}(s+1) + x'_{1,B}(s) + x'_{1,B}(s+1)] + \\ 4[&-x_{1,B}(s) + x_{1,B}(s+1) - x_{1,A}(s) + x_{1,A}(s+1)])/8, \end{aligned} \tag{36}$$

$$\begin{aligned} A_{22} = (\Delta X[&x'_{1,A}(s) - x'_{1,A}(s+1) + x'_{1,B}(s) - x'_{1,B}(s+1)] + \\ 6[&x_{1,A}(s) - x_{1,A}(s+1) + x_{1,B}(s) - x_{1,B}(s+1)])/4, \end{aligned} \tag{37}$$

$$\begin{aligned} A_{23} = (-\Delta X[&x'_{1,A}(s) + x'_{1,A}(s+1) + x'_{1,B}(s) + x'_{1,B}(s+1)] + \\ 6[&x_{1,B}(s) + x_{1,B}(s+1) - x_{1,A}(s) - x_{1,A}(s+1)])/8, \end{aligned} \tag{38}$$

$$\begin{aligned} A_{24} = (-\Delta X[&x'_{1,A}(s) + x'_{1,A}(s+1) + x'_{1,B}(s) + x'_{1,B}(s+1)] + \\ 6[&x_{1,B}(s) + x_{1,B}(s+1) - x_{1,A}(s) - x_{1,A}(s+1)])/8. \end{aligned} \tag{39}$$

By substituting the above formulae for the potential and kinetic energies we can express the action integral as a function of the displacements and its spatial derivatives at the corners of the element.

The action integral over the whole space and time domain is equal to the sum action integrals over the finite elements and is an algebraic expression. In the linear case it is a second order polynomial of all unknown quantities and should attain a stationary value. Thus, the partial derivatives with respect to the unknown displacements and spatial derivatives must be zero. These relations yield a system of algebraic equations for the unknown displacements $u(r,s)$, $x_2(r,s)$ and its spatial derivatives $x'_1(r,s)$, $x'_2(r,s)$.

For a typical point in the fluid these quantities appear in the action integrals only in four neighboring elements as shown in Fig. 2, where the elements are denoted by Roman numerals.

For a typical point (r,s), the unknown displacement $x_1(r+1,s)$ enters only in the four finite elements of its neighborhood. Let us denote the finite element with the corners $u(r,s)$, $u(r,s)$, $x_1(r+1,s+1)$ and $x_1(r,s+1)$ as I, and the consecutive finite elements when one moves clock-wise around the point (r, s) as II, III, IV. Generally, the algebraic equation corresponding to the typical point (r,s) is obtained by substituting the corresponding expressions to the action integral of the element. The same procedure has been applied for displacement $x_2(r,s)$ and values $x'_1(r,s)$, $x'_2(r,s)$.

For quantities $x'_1(r,s)$, $x'_2(r,s)$ and typical point on the left boundary $(0,s)$ the neighboring finite elements correspond to the elements denoted above as I and IV.

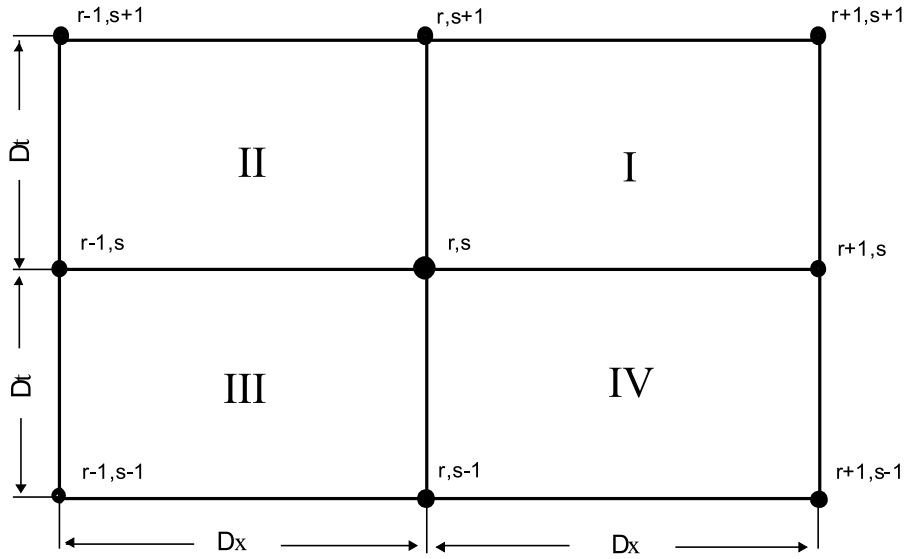

Fig. 2. Typical internal nodal point $r\Delta Z^1$, $s\Delta t$ and the adjacent finite elements I, II, III, IV

5. Experimental Verification

The results of numerical simulations have been compared with experimental data. The experiments were performed in the Institute of Hydro-Engineering in Gdańsk (Wilde, Chybicki 2000), in the flume 64 m long and 0.6 m wide. Depth of water during all experiments was 0.60 m. In every test the piston generator started smoothly from the rest. The position of the free surface was measured at seven points along the flume as a function of time and was acquired at 50 Hz. The first gauge was placed 8 m from the piston at rest and the last 8 m further, thus spacing between gauges was 1.33 m. The length of the wave group was chosen in such a way that the reflection from the end of the flume had no influence on the measured values. The measured displacements of the piston were used as the boundary condition in the numerical calculations. The generator was a piston-type, thus at the boundary the first component of horizontal displacement (independent of vertical variable) has the same position as the measured plate of the generator. The second component at the boundary is always zero.

Very important are boundary conditions for first spatial derivatives of both components of horizontal displacements. The conditions, that the variations of the derivatives are zero generate free waves with considerably higher amplitude than those observed in experiments in the flume. However, as shown in Fig. 2, at the boundary only two elements are taken into account, namely: I and IV. In the approach presented here, the boundary conditions for these quantities were assumed to be zero.

The calculation of non-linear effects was based on the fact that in each time step the solution of the non-linear problem is very close to the linear approach. Thus, in each time step the linear problem is solved and then, the non-linear correction is added. In the numerical code only the first order non-linearity was taken into account. The non-linearity is very strong in the vicinity of the generator and in this area the potential energy may be non-positive. As mentioned before, only part of the potential energy, dependent on term $(x_{1,X} + x_{2,X}/3)$, is controlled by linear contribution. In the numerical code only this part was considered:

$$Lp = 126(x_{1,X} + x_{2,X}/3)^3/1000. \tag{40}$$

The comparisons have been made for various amplitudes and ratios of wavelength to water depth equal to 4, 6, 8 and 12. The comparison between numerical simulations and experimental results for ratio $L/H = 4$ is shown in Fig. 3.

It can be seen that there exists quite good conformity between computed amplitudes and experiment data. However, calculated high frequency components, visible at the end of wave packets, are greater than those observed in the experiment. This effect occurred in all tested cases. The influence of non-linear terms manifests only in phase velocity, in which waves are faster as in linear case. In the case of the group velocity i.e. velocity of propagation of wave packet the agreement is also very good. The change of envelope arises from the dispersion – the shape of envelope is the same in linear and nonlinear cases.

Similar comparison was made for higher amplitudes, (Fig. 4). The agreement is also quite good. The shape of wave is more typical for the non-linear case – the crests of waves are narrow and high.

Figs. 5 and 6 illustrate the comparison between numerical and experimental results for wave packet with ratio $L/H = 6$. For this case, agreement between amplitudes and phases is still highly acceptable.

Similar conformity was obtained for high value of wave amplitude. It is a general property that if the wave is longer, the nonlinear dispersion i.e. the influence of nonlinearity on phase velocity is smaller while the influence on the shape of waves is greater.

For the ratio $L/H = 8$ linear and non-linear solutions are nearly the same. There is only one essential difference – in the non-linear case the high frequency harmonics are greater. Comparison of different amplitudes is presented in Figs. 7 and 8.

For long waves with the ratio $L/H = 12$ a comparison between experimental data and numerical solution is shown in Figs. 9 and 10. Note that in the second case the Ursell number is equal to 45 and non-linear and dispersional effects are comparable. It can be noted, that high frequency harmonics, propagating with different velocity, change the shape of waves.

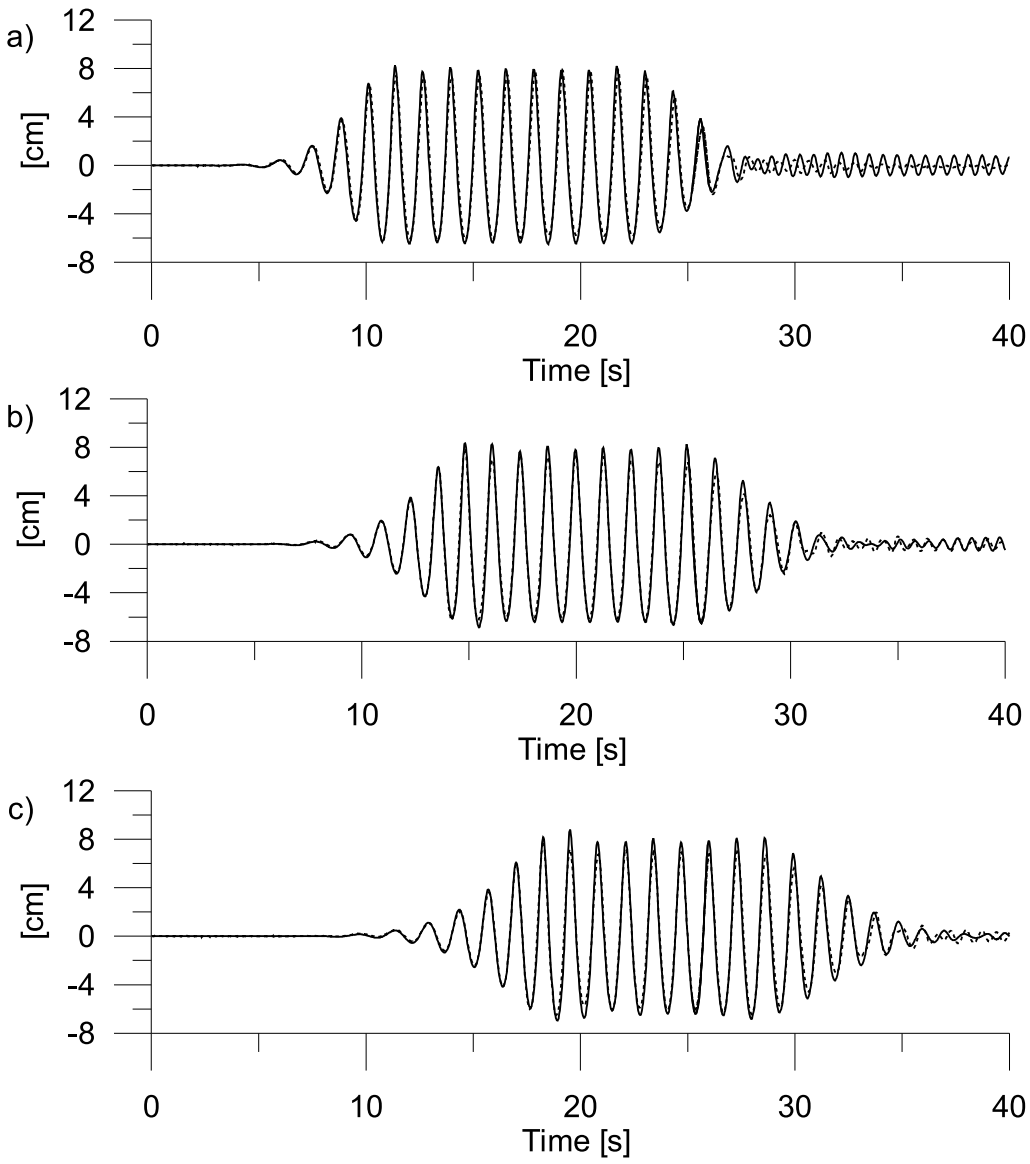

Fig. 3. Free surface elevation for wave with $L/H = 4$ at a) 8 m b) 12 m c) 16 m from generator. Wave height – 14 cm. Solid line – numerical calculations, dashed line – experiment

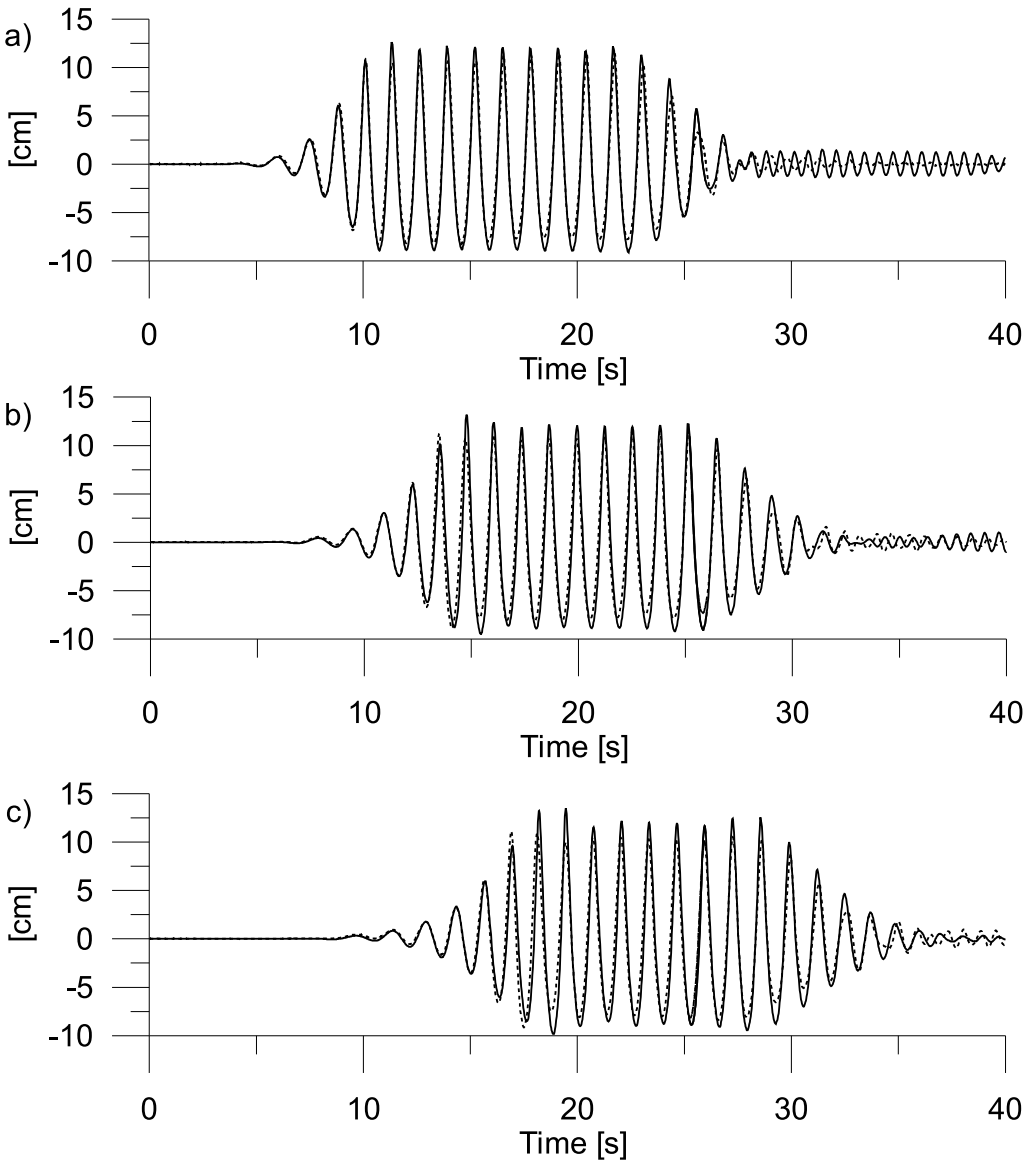

Fig. 4. Free surface elevation for wave with $L/H = 4$ at a) 8 m b) 12 m c) 16 m from generator. Wave height 20 cm. Solid line – numerical calculations, dashed line – experiment

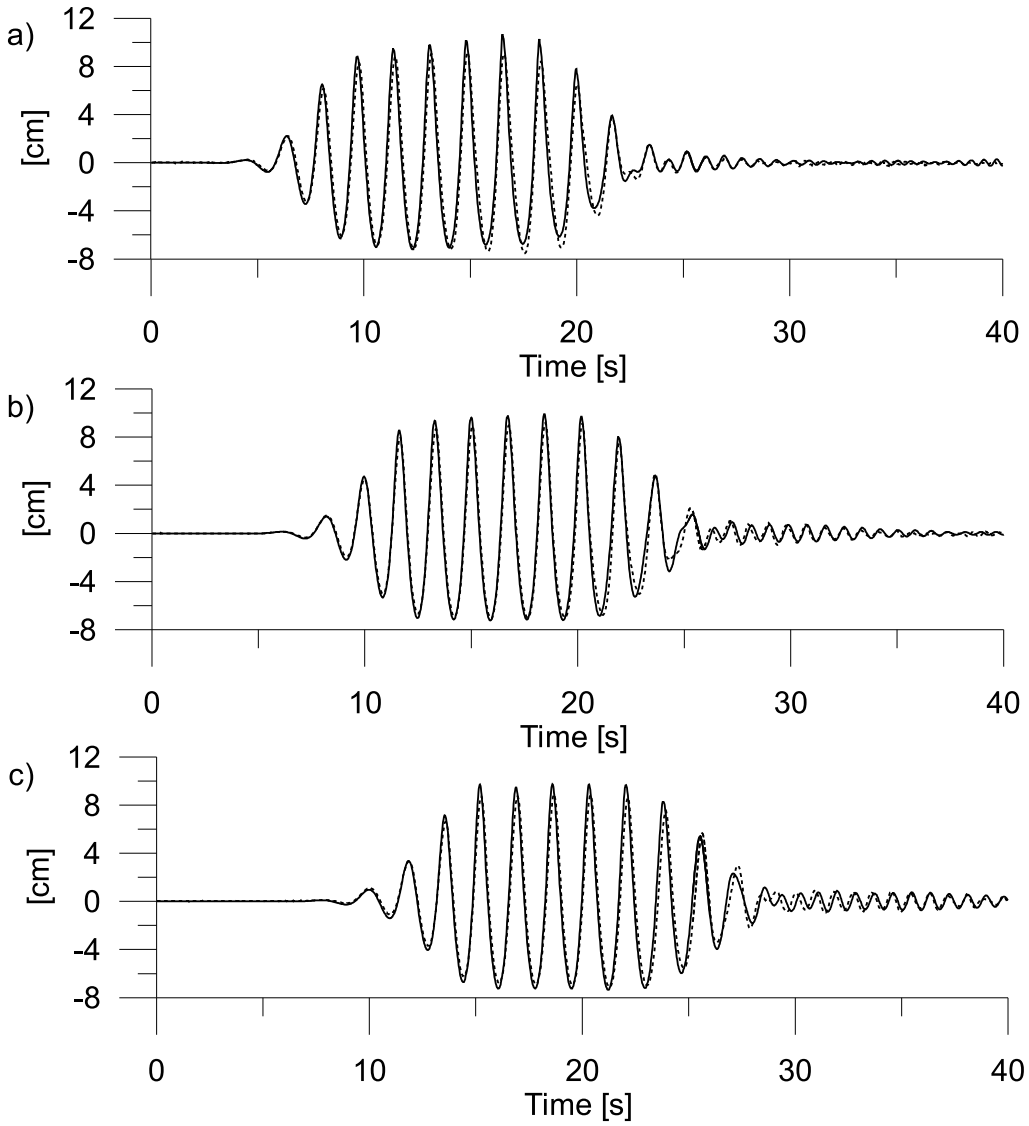

Fig. 5. Free surface elevation for wave with $L/H = 6$ at a) 8 m b) 12 m c) 16 m from generator. Wave height 16 cm. Solid line – numerical calculations, dashed line – experiment

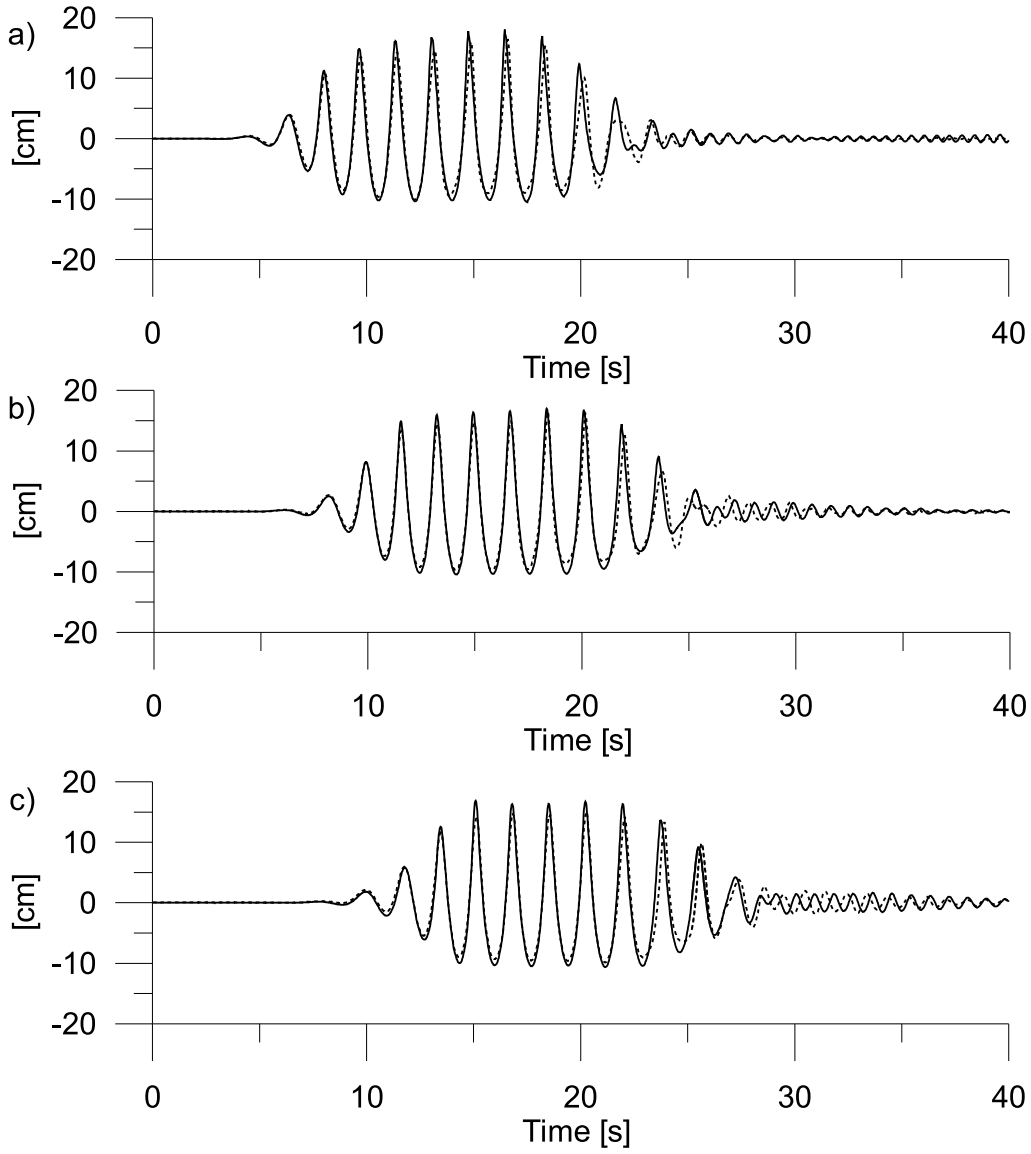

Fig. 6. Free surface elevation for wave with $L/H = 6$ at a) 8 m b) 12 m c) 16 m from generator. Wave height 28 cm. Solid line – numerical calculations, dashed line – experiment

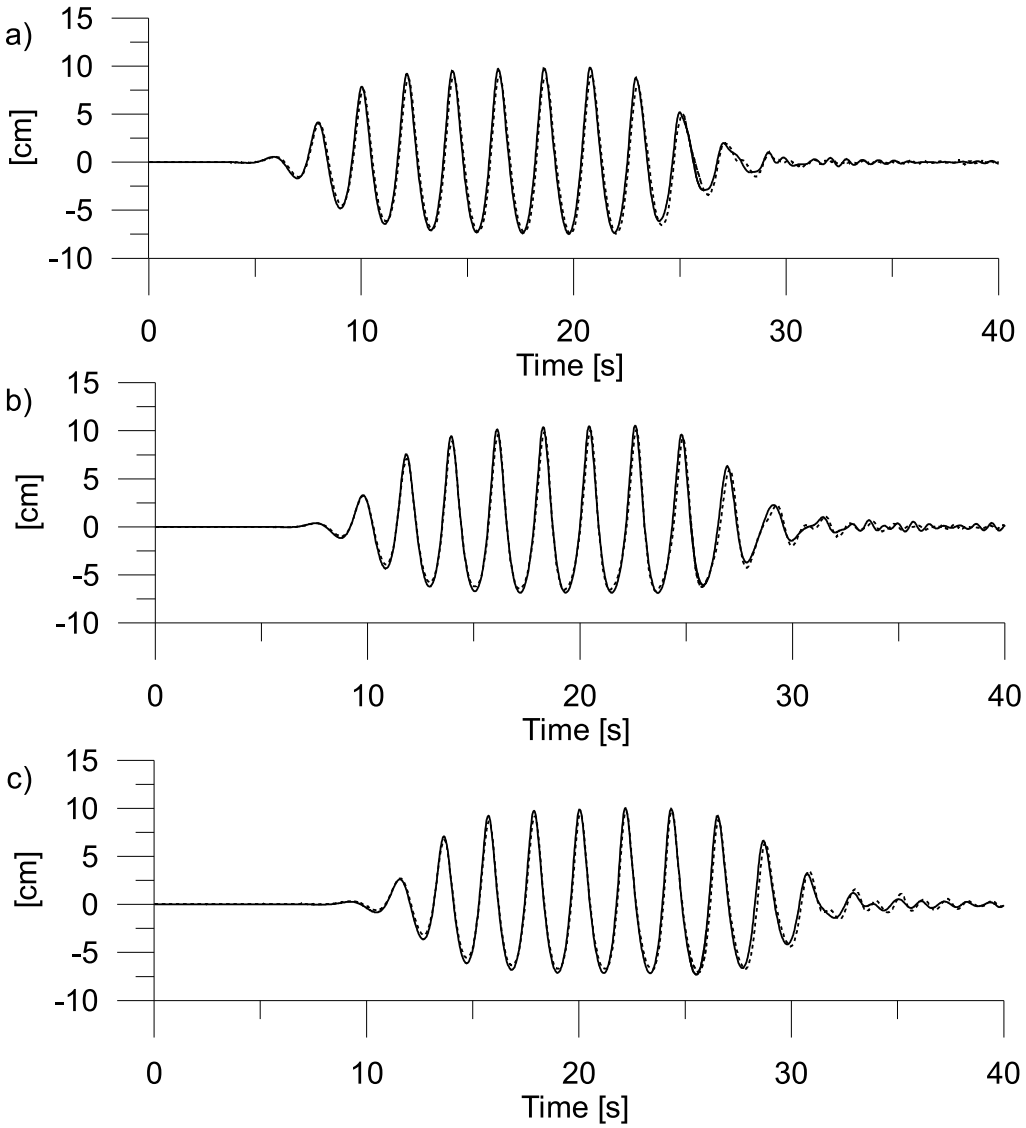

Fig. 7. Free surface elevation for wave with $L/H = 8$ at a) 8 m b) 12 m c) 16 m from generator. Wave height 15 cm. Solid line – numerical calculations, dashed line – experiment

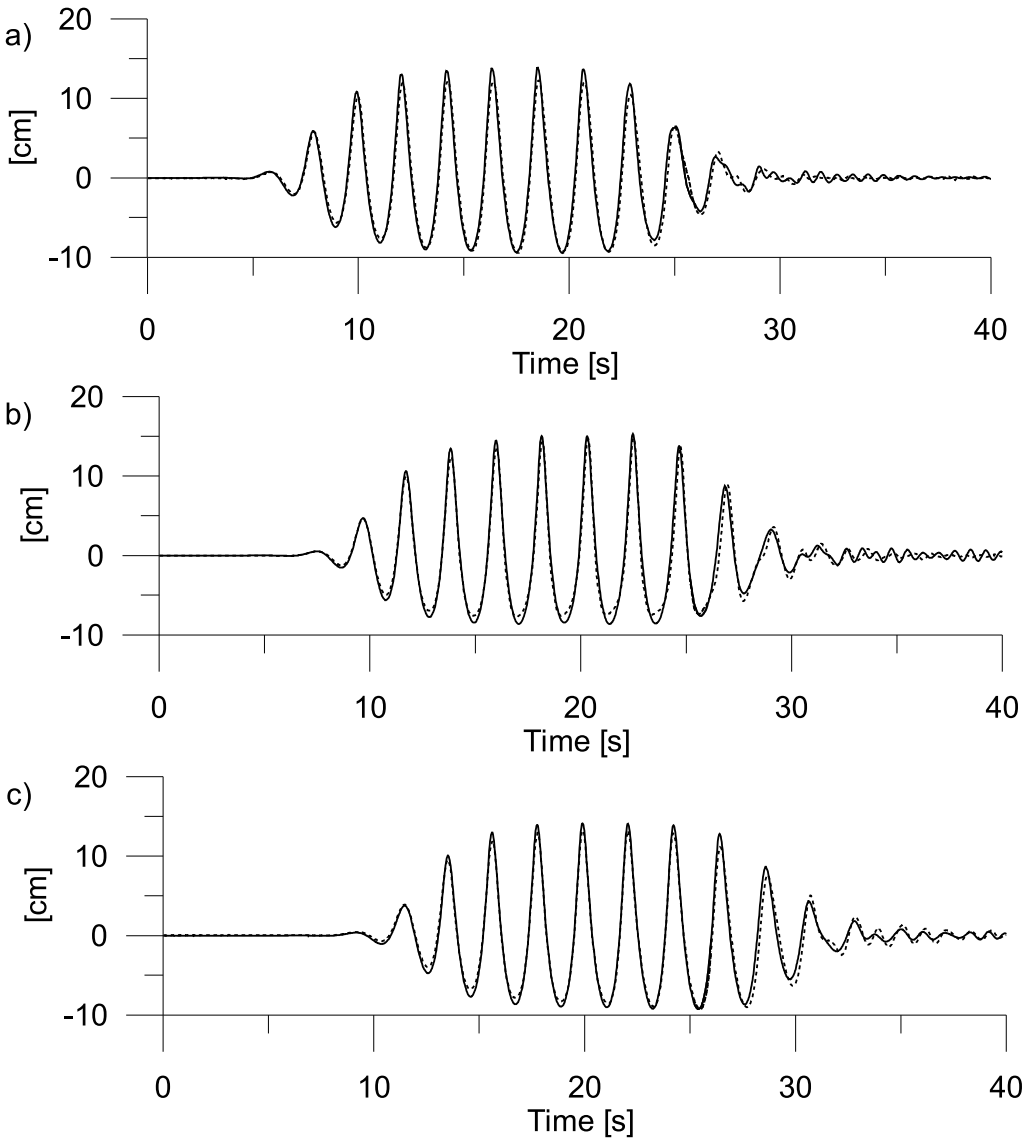

Fig. 8. Free surface elevation for wave with $L/H = 8$ at a) 8 m b) 12 m c) 16 m from generator. Wave height 26 cm. Solid line – numerical calculations, dashed line – experiment

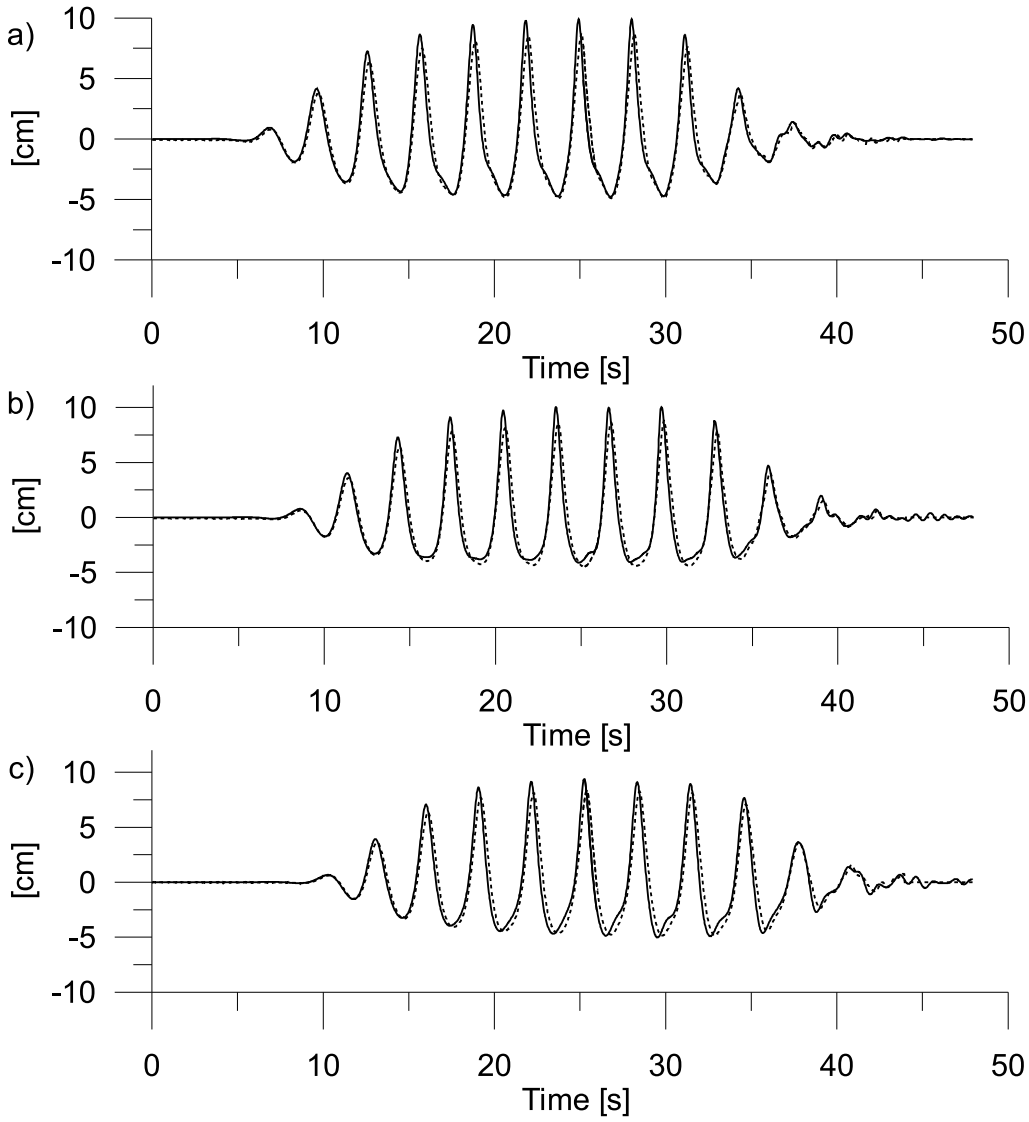

Fig. 9. Free surface elevation for wave with $L/H = 12$ at a) 8 m b) 12 m c) 16 m from generator. Wave height 14 cm. Solid line – numerical calculations, dashed line – experiment

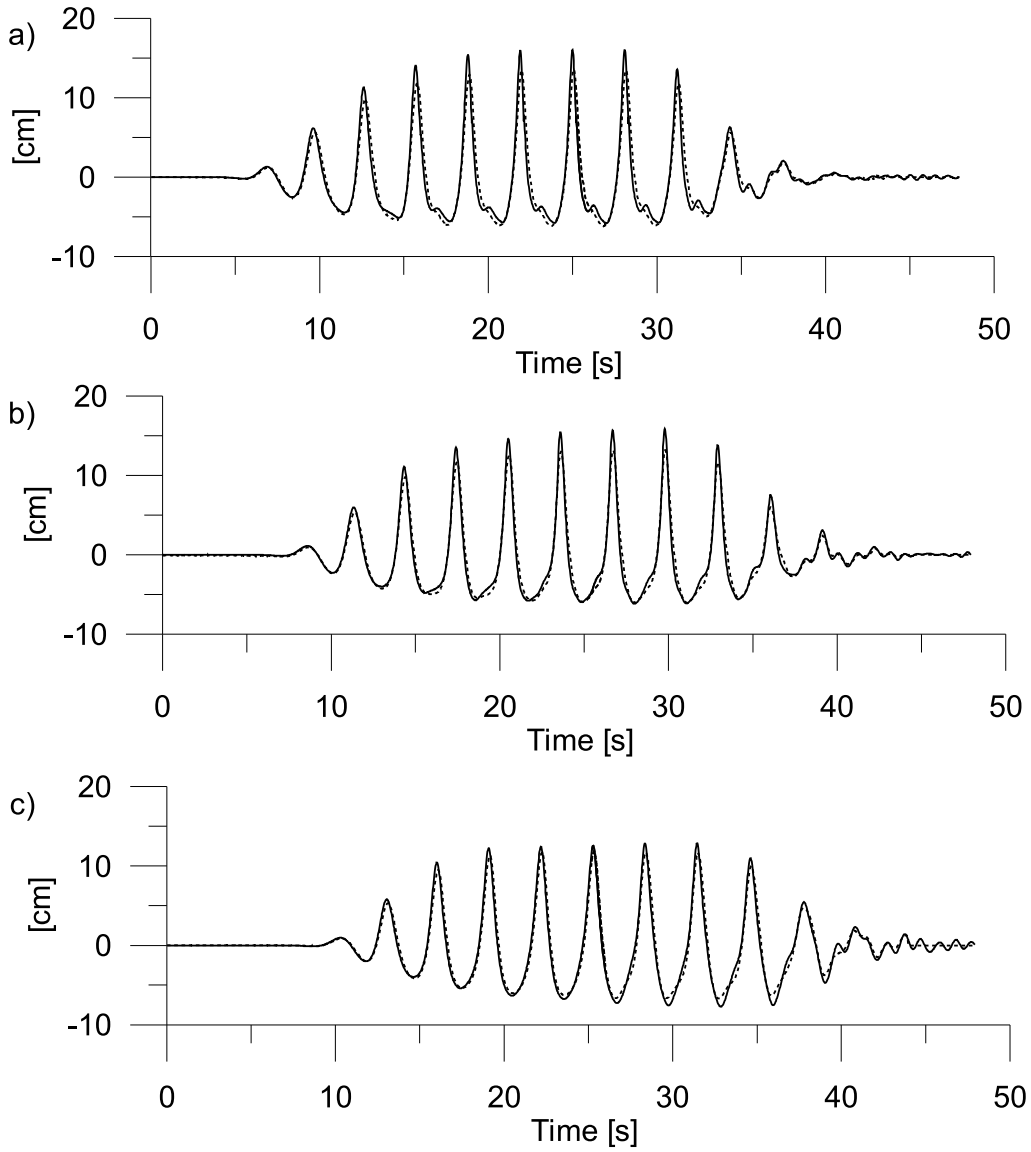

Fig. 10. Free surface elevation for wave with $L/H = 12$ at a) 8 m b) 12 m c) 16 m from generator. Wave height 22 cm. Solid line – numerical calculations, dashed line – experiment

6. Results and Conclusions

This paper deals with a form of equations describing water waves moving at finite depth. For the waves the introduced assumptions concerning the type of vertical displacement lead to the expressions for the kinetic and potential energies as functions of X and time t. Partial differential equations obtained from variational principle are independent of vertical variable Y. Corresponding dispersion relation is satisfied for a wide range of the ratio of wavelength to water depth.

A numerical solution of the equations is obtained and comparison with experimental data is shown. In the numerical model a shape function is assumed and the expressions for the potential and kinetic energies are derived. The energies are functions of horizontal displacements and their spatial derivatives at the nodal points. The action integral is an algebraic equation in terms of the unknown horizontal displacements and their derivatives.

The comparison of the experimental results with the calculated values shows good conformity with the case of a wavetrain with a dominant frequency for all waves with ratio L/H from 4 to 12. In numerical calculations higher free waves are obtained. In real situation there is a flow and there are boundary layers that introduce turbulence into the neighborhood of the piston. Thus, there must be a loss of energy in the generated waves.

For long waves the non-linear effects change the shape of waves while for shorter waves these effects focus on phase velocity. In the vicinity of a piston-type wave generator the motion of water particles is more complicated and probably cannot be described within the framework of the presented theory.

References

Chamberlain P. G., Porter D. (1995), The Modified Mild-Slope Equation, *J. Fluid Mech.*, **291**, 393–407.

Dingemans M. W. (1997a), *Water Wave Propagation over Uneven Bottoms*. Part 1 *Linear Wave Propagation*, Word Scientific Pub., Singapore.

Dingemans M. W. (1997b), *Water Wave Propagation over Uneven Bottoms*. Part 2 *Non-linear Wave Propagation*, Word Scientific Pub., Singapore.

Luke J. C. (1967), A Variational Principle for a Fluid with a Free Surfaces, *J. Fluid Mech.*, Vol. 27, 395–397.

Liu P. L.-F. (1995), Model Equations for Wave Propagation from Deep to Shallow Water, *Adv. in Coastal & Ocean Engineering*, 1, 125–157.

Madsen P. A., Murray R. & Sorensen O. R. (1991), A New Form of the Boussinesq Equation with Improved Linear Dispersion Characteristics, *Coastal Engineering*, 15, 371–388.

Massel S. R. (1989), *Hydrodynamics of Coastal Zones*, Elsevier, Amsterdam.

Peregrine D. H. (1967), Long Waves on Beach, *J. Fluid Mech.*, Vol. 27, 815–827.

Stoker J. J. (1957), *Water Waves*, Inter Science Publishers, New York.

Ursell F. (1953), The Long Wave Paradox in the Theory of Gravity Waves, *Proc. Cambridge Philos. Soc.*, 49.

Wei G., Kirby J. T., Grili S. T., Subramanya R. (1995), A Fully Nonlinear Boussineq Model for Surface Waves: Part 1. Highly Nonlinear Unsteady Waves, *J. Fluid Mech.*, 294, 71–92.

Wei G., Kirby J. T., Sinha A. (1999), Generation of Waves in Boussinesq Models Using a Source Function Method, *Coastal Engineering*, Vol. 36, No. 4, 271–299.

Wilde P., Chybicki W. (2000), *Numerical Solution for Long Waves in Lagrange's Description* (in Polish), Internal Report of IBW PAN.

Whitham G. B. (1974), *Linear and Non-linear Waves*, J. Wiley & Sons, New York.